

The Opposed-Piston Engine: The Next Step in Vehicle Efficiency

Dr. Gerhard Regner, Achates Power, Inc., San Diego, CA;
Dr. Ashwin Salvi, Achates Power, Inc., San Diego, CA;
Laurence Fromm, Achates Power, Inc., San Diego, CA;
Fabien Redon, Achates Power, Inc., San Diego, CA

Abstract

Vehicle and engine manufacturers face a daunting challenge of meeting future emissions and fuel economy standards in a cost effective manner. Compliance with these regulations requires significant financial investments in new technologies, all designed to increase fuel efficiency while decreasing emissions.

One solution to this problem is the opposed-piston engine. Achates Power has spent the past 12 years modernizing this historically efficient engine architecture to deliver a step-wise improvement in brake thermal efficiency (BTE) over the most advanced conventional four-stroke engines. In addition, with the elimination of parts such as the cylinder head and valve train, it is also less complex and less costly to produce - making it even more appealing to manufacturers.

Measured steady state results from the 13-mode Supplemental Emissions Test (SET) cycle on the Achates Power research grade three-cylinder, 4.9L opposed-piston engine equipped with a two-speed supercharger demonstrate the ability of the technology to achieve high fuel efficiency while satisfying emissions criteria. The SET cycle average of 199 g/kWh, with a best point of 190 g/kWh, highlights the flat nature of the fuel map. With an optimized, production intent engine design, an estimated 180 g/kWh SET cycle average is expected. Work with Johnson Matthey and their patented Selective Catalytic Reduction Technology (SCRT[®]) system has shown that the Achates Power OP Engine can satisfy HC, CO, PM, and NO_x U.S. EPA10 emissions over the SET cycle [1].

Initial transient results are encouraging with cycle averaged BSFC similar to steady-state BSFC, and engine out emissions compliant with regulatory standards when coupled with commercially available after-treatment equipment [2]. These results highlight the capabilities of the opposed-piston engine to perform transient maneuvers successfully without compromising fuel economy and emissions.

Light-duty estimations of the OP Engine simulated in a pickup truck suggest a 30% improvement in fuel economy over an efficiency-optimized, four-stroke diesel research engine [3]. Results show that with the OP Engine, 2025 CAFE regulations for light-duty trucks can be met and superseded without any advanced vehicle level solutions. Achates Power is also working on developing a 2.7L Opposed-

Piston Gasoline Compression Ignition (OPGCI) engine, largely funded by the U.S. Department of Energy, ideal for light-duty applications [4]. The OPGCI technology has the potential to cost-effectively deliver more than 50% improved fuel economy over conventional gasoline engines while maintaining low emissions.

Introduction

Compliance with Euro 6, and U.S. Tier 3/LEV III, and U.S. HD GHG Phase 2 regulations requires significant financial investments in new technologies, all designed to increase fuel efficiency and decrease emissions with the side effect of increasing vehicle cost. However, to remain competitive, manufacturers cannot pass along these costs to fleet owners.

One cost-effective solution to stricter regulations is the opposed-piston engine. This engine, which has been optimized by Achates Power, was once widely used in a variety of applications including commercial vehicles, aviation, maritime and military vehicles. After overcoming the architecture's historical challenges, the Achates Power Opposed-Piston Engine (OP Engine) now delivers a step-wise improvement in BTE over the most advanced conventional four-stroke engines. In addition, with the elimination of parts such as the cylinder head and valve train, it is also less complex and less costly to produce—making it even more appealing to manufacturers.

Thermodynamics and Heat Transfer Advantages of Opposed-Piston Engines

Produced initially for their manufacturability and high power density, opposed-piston, two-stroke engines have demonstrated superior fuel efficiency compared to their four-stroke counterparts. This section examines the underlying reasons for the superior fuel efficiency and emissions.

Reduced Heat Losses

The Achates Power Opposed-Piston Engine, which includes two pistons facing each other in the same cylinder, offers the opportunity to combine the stroke of both pistons to increase the effective stroke-to-bore ratio of the cylinder. As a thought experiment, when a two cylinder conventional engine with 1.1 stroke-to-bore is re-architected as a single-cylinder opposed-piston engine with both pistons operating in the same bore, it results in an OP Engine with 2.2 stroke-to-bore ratio. This can be accomplished while maintaining the engine and piston speed of the conventional four-stroke engine. To achieve the same stroke-to-bore ratio with a conventional four-stroke engine, the mean piston speed would double for the same engine speed. This would severely limit the engine speed range and, therefore, the power output. The increase in stroke-to-bore ratio has a direct mathematical relationship to the area-to-volume ratio of the combustion chamber volume. Figure 1 shows the

comparison of a conventional four-stroke engine to an opposed-piston engine with the same piston and crank dimensions in regards to area-volume as a function of engine displacement. In this example, the reduction in the surface area to volume ratio is a very significant 36%. A 6L opposed-piston engine has equivalent area-to-volume ratio as a 15L conventional engine. The lower surface area directly leads to a reduction in heat transfer. An additional benefit of the reduced heat losses in the opposed-piston engine, especially for commercial vehicles, is the reduction in fan power and radiator size, further contributing to vehicle level fuel savings.

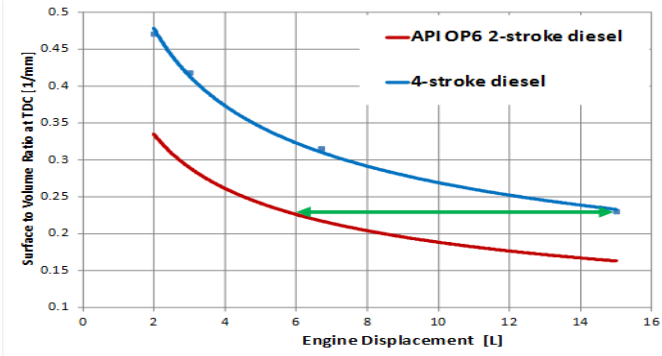


Figure 1: Surface area to volume ratio as a function of engine displacement for opposed-piston and conventional engines

Leaner Combustion

When configuring an opposed-piston, two-stroke engine of the same displacement as a four-stroke engine –for example, converting a six-cylinder, conventional engine into a three-cylinder, opposed-piston engine – the power that each cylinder has to deliver is the same. The opposed-piston engine fires each of the three cylinders in each revolution while the four-stroke engine fires each of its six cylinders in one out of two revolutions. Therefore, the amount of fuel injected for each combustion event is similar, but the cylinder volume is 60% greater for the Achates Power OP Engine. So for the same boost conditions, the OP Engine will achieve leaner combustion, which increases the ratio of specific heat. Increasing the ratio of specific heat increases the work extraction per unit of volume expansion during the expansion stroke.

Near Constant Volume Combustion

The larger combustion volume for the given amount of energy released also enables shorter combustion duration while preserving the same maximum pressure rise rate and peak cylinder pressure. The faster combustion improves thermal efficiency by reaching a condition closer to constant volume combustion. The lower heat losses as described above lead to a 50% burn location closer to the minimum volume. Figure 2 illustrates how the heat release rate compares between a four-stroke engine and the Achates Power OP Engine. Ideal combustion should occur at minimum

volume and occur at constant volume. The OP Engine is much closer to this ideal condition at the same pressure rise rate and peak cylinder pressure.

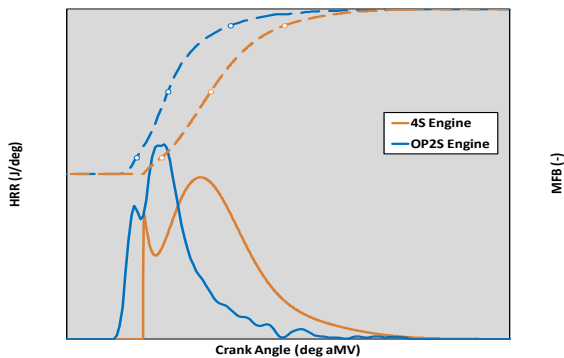


Figure 2: Heat release rates and mass fraction burned for opposed-piston 2 stroke and conventional engines

The aforementioned fundamental opposed-piston, two-stroke (OP2S) thermal efficiency advantages [5] are further amplified by:

- Lower heat loss due to higher wall temperature of the two piston crowns compared to a cylinder head (reduced temperature difference)
- Reduced pumping work due to uniflow scavenging with the OP2S architecture resulting in higher effective flow area than a comparable four-stroke or a single-piston two-stroke uniflow or loop-scavenged engine
- Decoupling of pumping process from the piston motion because of the two-stroke architecture allows alignment of the engine operation with a maximum compressor efficiency line

Key Enablers for Opposed-Piston Engine Efficiency and Emissions

Combustion System

Achates Power has developed a proprietary combustion system [6] composed of two identical pistons coming together to form an elongated ellipsoidal combustion volume where the injectors are located at the end of the long axis [7] (Figure 3).

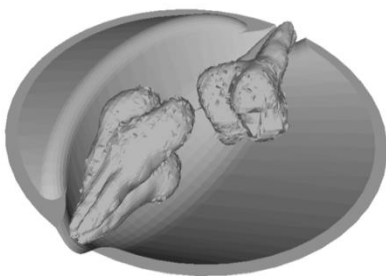


Figure 3: Schematic of side-mounted injectors in combustion chamber

This combustion system allows the following:

- High turbulence, mixing and air utilization with both swirl and tumble charge motion with the high turbulent kinetic energy available at the time of auto ignition
- Ellipsoidal combustion chamber resulting in air entrainment into the spray plumes from two sides
- Inter-digitated, mid-cylinder penetration of fuel plumes enabling larger $\lambda=1$ iso-surfaces
- Excellent control at lower fuel flow rates because of two small injectors instead of a single higher flow rate
- Multiple injection events and optimization flexibility with strategies such as injector staggering and rate-shaping [7]

The result is no direct fuel spray impingement on the piston walls and minimal flame-wall interaction during combustion. This improves performance and emissions [8] with fewer hot spots on the piston surfaces that further reduce heat losses [7].

Air System

To provide a sufficient amount of air for combustion, two-stroke engines need to maintain an appropriate pressure difference between the intake and exhaust ports. For applications that require the engine to change speed and load in a transient manner, such as automotive applications, external means of air pumping are required. Among the various possible configurations of the air system with turbocharger and supercharger combinations, the layout as described in Figure 4 is the preferred configuration [9].

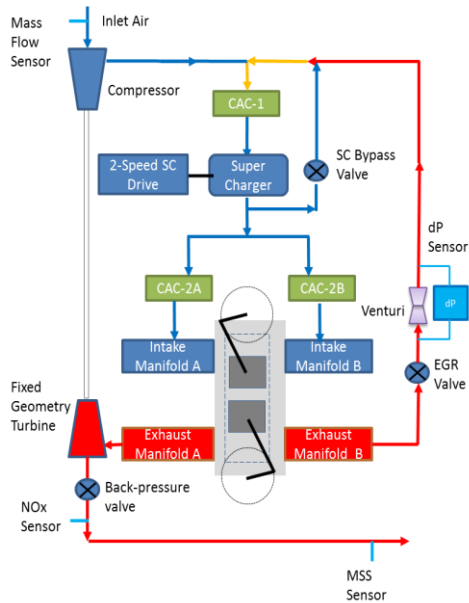


Figure 4: One example schematic of the Achates Power opposed-piston 2 stroke air system

Advantages of such an air system are summarized as follows:

- The compressor provides high pressure before the supercharger, which is further boosted by the supercharger. This means that low supercharger pressure ratios are sufficient for high intake manifold density, reducing pumping work.
- The maximum required compressor pressure ratio is lower compared to regular turbo-only air systems of four-stroke engines.
- The use of a supercharger recirculation valve allows greater control of the flow through the engine, thus providing flexibility for precise control of boost, scavenging ratio, and trapped residuals to minimize pumping work and NO_x formation across the engine map
- Lowering the flow through the engine by decreasing the pressure difference across the engine reduces the pumping penalty at low load points. This, together with having no dedicated intake and exhaust stroke for moving mass from and to the cylinder improves BSFC.
- A two-speed supercharger drive and recirculation valve improves transient response and air control over the engine map [10].
- Accurate control of the engine pressure differential provides very good cold start and catalyst light off capabilities [11]. Low-speed torque is increased by selecting the appropriate gear ratios on the supercharger [8].
- Driving exhaust gas recirculation (EGR) with a supercharger reduces the required pumping work [8].

- Mixing of cool air and EGR together before the charge air cooler reduces fouling [8, 12].

Multi-Cylinder Opposed-Piston Engine and Research Platform Specifications

Engine Specifications

A multi-cylinder platform, A48-316, was used to generate the results presented in this paper. This multi-cylinder research engine was designed to meet the performance levels shown in Table 1.

Table 1: Achates Power A48-316 Opposed-Piston two-stroke engine specifications

Displacement	4.9 L
Arrangement, number of cylinders.	Inline 3
Bore	98.4 mm
Displaced Stroke	215.9 mm
Stroke-to-Bore Ratio	2.2
Compression Ratio	15.4:1
Nominal Power (kW @ rpm)	205 @ 2200
Max. Torque (Nm @ rpm)	1100 Nm @ 1200-1600
Emission level	U.S. 2010/ Euro 6

This engine was conceived as a research test platform and it utilizes oversized components and systems to provide a significant level of flexibility required for exploring the capabilities of the engine. As a result, the size of the engine and the friction that has to be overcome is higher than expected from an optimized production engine.

Figure 4 provides an overview of the air-path for the three-cylinder diesel Achates Power Opposed-Piston Engine. Upstream of the OP Engine, a compressor driven by fixed-geometry turbo is used to draw in fresh air. To aid the airflow across the engine, there is a supercharger driven by a two-speed drive that allows it to run at two different supercharger-to-engine speed ratios. For this engine, two drive ratios that were used are 3.2 and 4.6. A supercharger recirculation valve is used to control the airflow across the engine. The supercharger also creates positive differential pressure across the EGR loop to drive flow from exhaust manifold to compressor outlet. A venturi in the EGR loop with a delta-pressure sensor mounted across it is used to measure the EGR mass-flow. EGR valve is used to control the EGR flow to the engine. Downstream of the engine, a back-pressure valve is used to maintain the back-pressure of a clean after-treatment system.

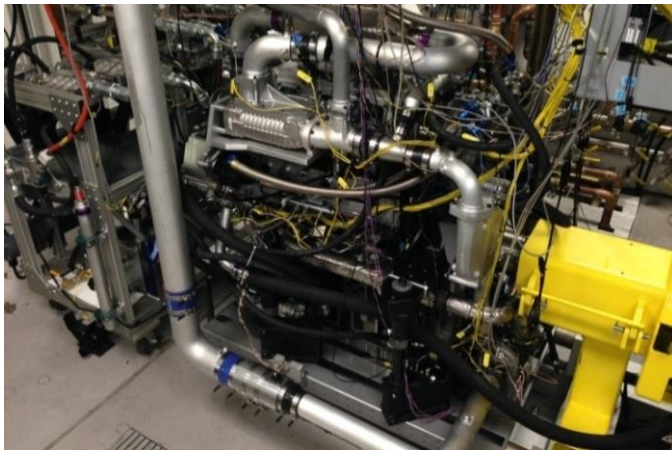


Figure 5: A48-316 in test cell

Dynamometer System and Test Cell instrumentation

The dynamometer system consists of a SAJ SE-400 eddy current absorber unit with a capacity of 400kW and 2000Nm. The inertia offered by the dyno is $0.82\text{kg}\cdot\text{m}^2$. The engine is coupled to the absorber with a Cardan shaft of 10,000Nm capacity. The speed-control loop of the dynamometer is executed at a frequency of 200Hz. Since this is an absorbing dynamometer, it is not possible to execute the motoring portion of the any test cycle. During such instances of the cycle, 10% of the brake-torque relative to the engine speed is commanded. Unlike a transient dynamometer, this dynamometer does not support closed-loop torque control to meet torque set-points. Torque profile is forwarded to ECU over CAN and ECU software has a torque-to-fuel map that generates fuel command to meet desired torque. Torque is measured by a Honeywell torque sensor (TMS9250) which is capable of measuring from 0 Nm to 4000Nm with an accuracy of $\pm 4\text{Nm}$. The torque flange is mounted in the driveline between the engine and the dyno-absorber. Zero-offset correction is performed before the test to account for any drift in the sensor measurement. Soot was measured using real-time AVL483 micro soot sensor. The soot number reported by AVL483 corresponds to elemental carbon content of total particulate mass. Engine out NO_x was measured using both FTIR (for steady state operation) and real time Continental NO_x sensor (for transient operation). Other gaseous emissions (HC and CO) were also measured using MKS FTIR. The NO_x numbers reported in the results section are as measured by the emission bench and have been corrected for humidity as per EPA CFR 40 part 1065.

Multi-Cylinder Steady State Results

Results from steady state testing are shown in Table 2. The engine shown in Figure 5 is designed to be a robust research platform and therefore suffers for higher inertial and frictional losses. Despite this

disadvantage, the fuel consumption while meeting U.S. EPA 2010 emissions standards is still significantly lower compared to a conventional four stroke engine.

The averaged results of a 13-mode SET cycle are shown in Table 3. The difference of only 8 g/kWh between the cycle averaged BSFC of 199 g/kWh and the best point of 190 g/kWh highlights the flat nature of the BSFC map (Figure 6) and the advantage of improved real world fuel economy with the OP Engine. With an optimized, fresh design of the 4.9L engine, cycle averaged fuel consumption is expected to improve to 180 g/kWh and a best point of 176 g/kWh.

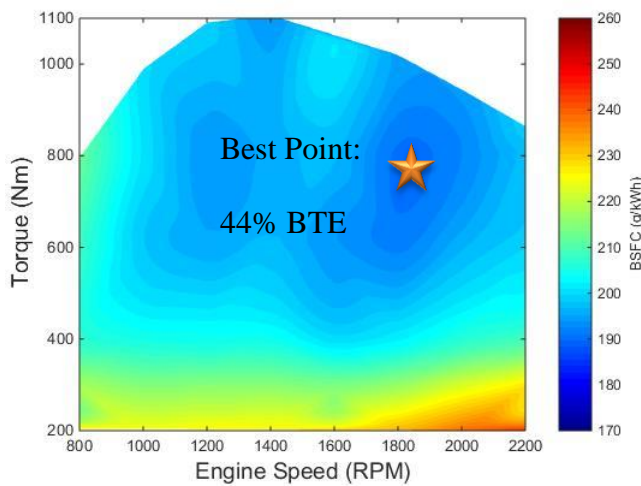


Figure 6: Measured BSFC map of the A48-316 engine

Measured BSSoot and BSNO_x maps are shown in Figure 7 and Figure 8 respectively, highlighting the low emissions capability of the Achates Power A48-316 engine.

Table 2: SET 13 mode results

		Idle	A25	A50	A75	A100	B25	B50	B75	B100	C25	C50	C75	C100
Speed	RPM	799.9	1400	1400	1400	1400	1800	1800	1800	1800	2200	2200	2200	2200
Torque	Nm	7.8	290.8	550.7	824.5	1091.0	267.5	527.6	781.8	1018.6	228.5	444.9	665.3	882.2
Brake Power	kW	0.7	42.7	80.8	120.9	160.0	50.4	99.5	147.4	192.1	52.7	102.5	153.3	203.4
BSNO _x	g/kWh	-	2.2	3.9	4.1	4.0	2.5	3.8	3.9	4.9	2.0	2.6	2.3	2.0
BSSoot	g/kWh	-	0.04	0.01	0.02	0.03	0.04	0.01	0.01	0.02	0.04	0.03	0.02	0.04
BSCO	g/kWh	-	0.6	0.3	1.1	3.1	0.7	0.2	0.8	2.4	0.7	0.3	0.3	1.3
BSHC	g/kWh	-	0.1	0.1	0.1	0.1	0.1	0.1	0.1	0.1	0.1	0.1	0.1	0.1
Air/Fuel Ratio	-	101.8	30.7	32.1	27.6	25.6	34.7	29.3	24.5	22.8	32.5	30.1	25.5	22.5
EGR rate	%	35.5	30.5	30.4	28.8	27.1	30.1	26.3	26.1	21.6	31.8	30.8	31.6	29.3
Turbine Out Temp	deg C	150.5	260.4	256.4	291.5	312.5	235.8	276.0	320.6	356.5	250.5	253.3	287.0	327.9
Turbine Out Pressure	bar A	1.0	1.03	1.06	1.10	1.14	1.05	1.08	1.11	1.16	1.06	1.09	1.13	1.17

Table 3: SET 13 mode averaged results

13 Mode SET Cycle Results		
Cycle Average Results		
BSNO _x	3.89	g/kW-hr
BSSoot	0.014	g/kW-hr
BSCO	0.81	g/kW-hr
BSHC	0.09	g/kW-hr

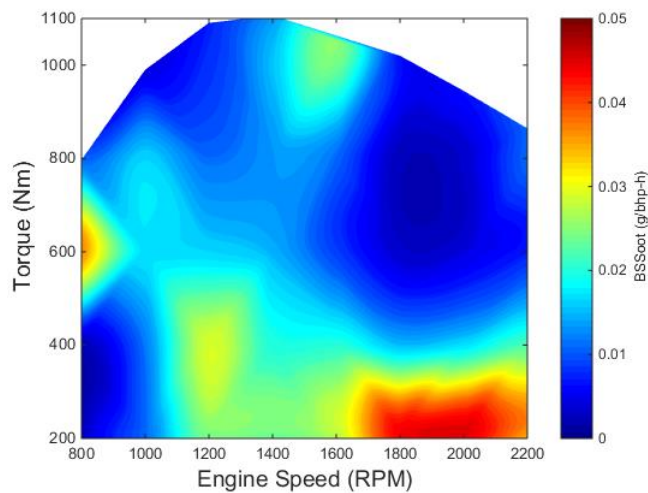


Figure 7: Measured BSSoot on the A48-316 engine

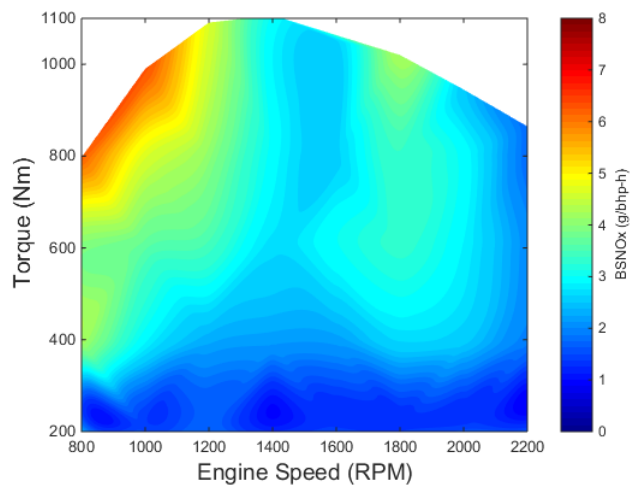


Figure 8: Measured BSNO_x on the A48-316 engine

To determine the ability of the OP Engine to satisfy emissions regulations, an after-treatment study was performed.

After-treatment Results

Work performed with Johnson Matthey and their patented SCRT® evaluated the potential of the OP Engine to satisfy emissions regulations, described in further detail in [1]. The four-way emissions control system utilizes a diesel oxidation catalyst (DOC) followed by a catalyzed soot filter (CSF), SCR catalyst, and finally an ammonia slip catalyst (ASC), as shown in Figure 9, to mitigate HC, CO, PM, NO_x, and NH₃ emissions.

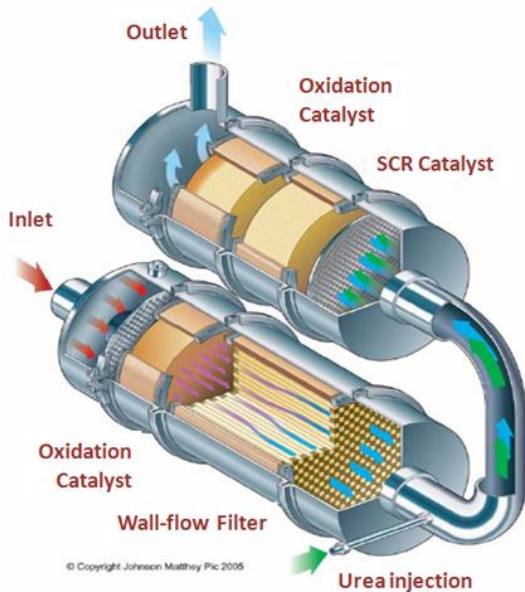


Figure 9: Johnson Matthey's SCRT® system

The first component is the diesel oxidation catalyst with platinum group metals - PGM (Pt or Pd) to oxidize HC and CO in the exhaust. In addition, the DOC plays an important role in both attaining passive regeneration for the DPF and high NO_x reduction in the downstream catalysts by oxidizing NO to NO₂. The second component is the catalyzed soot filter to remove particulate matter from the exhaust stream. The filter is coated with PGM to improve NO oxidation and in turn improve passive soot oxidation. PGM in the filter also helps in further oxidizing HC and CO that slips out of the DOC during active regeneration or high space velocity conditions. Filter substrate properties are to be chosen carefully for good ash capacity and Particle Number (PN) regulations. The third component is a selective reduction catalyst which has been proven effective in reducing NO_x. Urea is used as a reductant which hydrolyzes to produce NH₃. When the inlet NO₂/NO_x is high (50%), fast SCR reaction takes place instantaneously at temperatures >200°C leading to significantly high NO_x conversion [13]. Although stoichiometric amount of NH₃ is required to reduce NO_x, due to the NH₃ storage functionality in the catalyst and due to the dynamic nature of the feed conditions, urea is usually over injected into

the SCR catalyst to increase NO_x conversion. This results in NH_3 slip from the SCR catalyst. Hence a fourth component, the ammonia slip catalyst, is used to oxidize the excess NH_3 selectively to N_2 . The sizing of these four components, the formulation type and PGM loading in the DOC and the CSF are to be optimized for a given application to satisfy the emissions regulation limits.

Fully developed and validated high fidelity models have been utilized for the DOC, coated Filter (CSF), SCR (Cu- based), and ASC (Cu- based) formulations in this study. The DOC, SCR, and CSF models were developed using a 1D modeling framework with the CSF utilizing a single channel pair model that consisted of two parts: i) axial flow in the channels, and temperature effects in the filter; and ii) soot accumulation and removal, NO oxidation within the filter wall, and NO_2 diffusion from the wall to the soot cake. A 1D+1D model was developed for the selective Cu- based ammonia slip catalyst. Complex chemical kinetics were developed for each formulation to capture the catalyst behavior at both spatial and temporal coordinates and at varied feed conditions. Johnson Matthey has published a number of previous works on their state-of-the-art modeling efforts on gasoline and diesel applications; additional details about the frameworks used in this study can be found in the following references (DOC [14], CSF [15], SCR [16], and ASC [17]). A selection of modeling assumptions are listed here:

- 1) Uniform flow distribution at the monolith entrance
- 2) Negligible radial concentration and temperature profiles
- 3) Transport of mass and energy in the gas by convection
- 4) Transport of energy in the solid by conduction
- 5) Description of the transfer of mass and energy between the gas and the solid uses coefficients derived from a correlation available in the literature [18]
- 6) No diffusion resistance is present in the catalyst washcoat

The specifications for the after-treatment system components are shown in Figure 10. Using the engine out conditions from the SET cycle shown in Table 2, the results for the after-treatment system are shown in Figure 11. Each mode was simulated for 120 seconds, followed by a transition to the next mode over the course of five seconds.

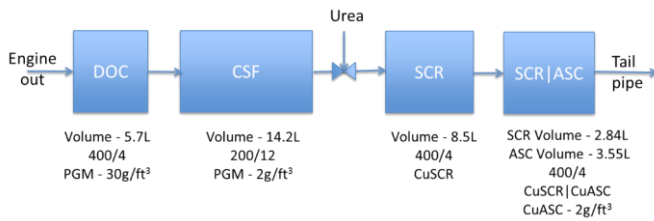


Figure 10: After-treatment component specifications

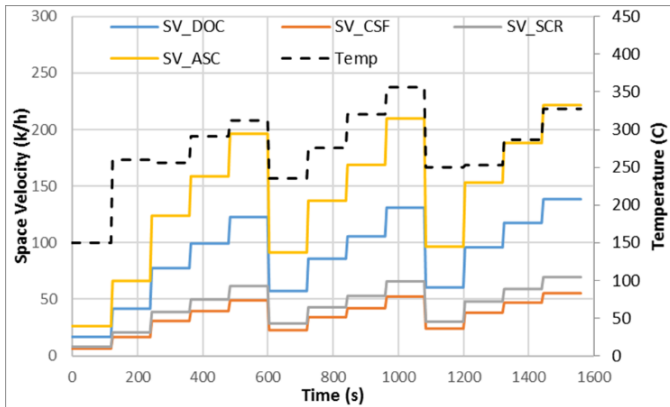


Figure 11: After-treatment temperatures and space velocities for the A48-316 13 mode SET cycle

Two Pt:Pd ratio cases were analyzed for the DOC: Case 1) 2:1 Pt:Pd ratio aged at 780C for 10 hours and Case 2) 5:1 Pt:Pd ratio aged at 700C for 100 hours. The two PGM loadings were selected to investigate the effect of NO₂/NO_x on soot oxidation and NO_x reduction, on top of HC and CO oxidation. A high Pt:Pd ratio oxidizes NO to NO₂ more rapidly in the DOC, leading to higher NO₂/NO_x ratios that assist in the passive regeneration of the CSF.

For this study, the HC speciation was assumed to be 74% Decane, 4% Toluene, and 22% Propylene. Figure 12 shows that CO oxidation is 100% for both cases as the exhaust temperature during the test cycle was higher than the light off temperature for the DOC. A slight improvement in HC oxidation was noticed for Case 2, the higher Pt:Pd ratio case, which results from higher Decane decomposition due to higher Pt loading.

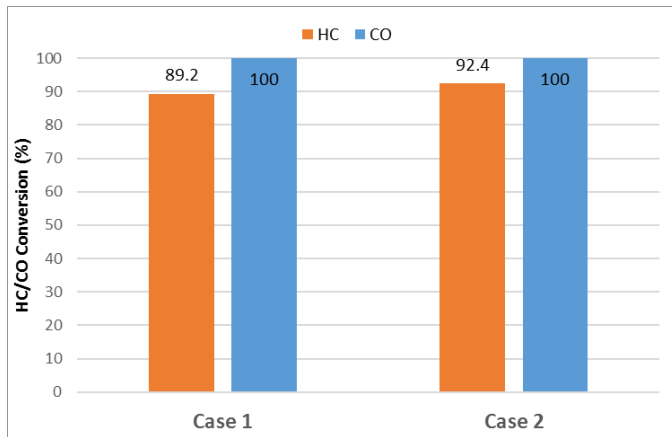


Figure 12: CO and HC oxidation across DOC and CSF during the 13-mode SET cycle

Assuming an engine-out NO_2/NO_x of 10%, Figure 13 shows that the NO_2/NO_x ratio is indeed higher for the higher Pt:Pd ratio (Case 2) resulting from increased NO oxidation. The CSF contains PGM that further converts NO from the DOC outlet into NO_2 , resulting in an increase in the NO_2/NO_x ratio. The higher NO_2/NO_x ratio assists in the passive oxidation of soot in the CSF, as shown by decreased soot loading for Case 2 in Figure 14. As a comparison, an uncoated particulate filter was also analyzed using the NO_2/NO_x outlet from Case 1. An increase in PGM loading of the CSF can aid in NO and soot oxidation, however the loading density needs to be optimized for the appropriate NO_2/NO_x DOC outlet ratio.

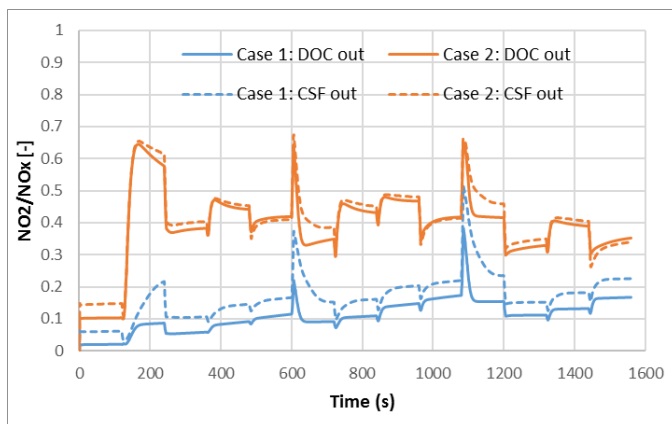


Figure 13: NO_2/NO_x ratio over the DOC and CSF during the 13-mode SET cycle

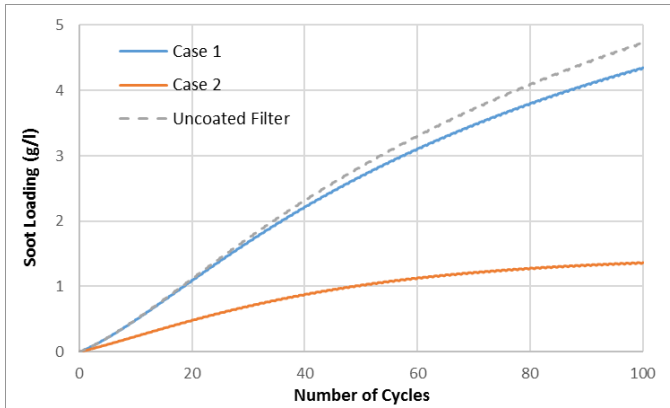


Figure 14: CSF soot loading for zero (Uncoated filter), low (Case 1), and high (Case 2) Pt:Pd ratios

NO_x reduction is handled through the urea SCR system, where the urea hydrolyzes to produce NH₃ and subsequently reduces NO and NO₂ via the standard, fast, and slow reactions source [13]. The SCR system is selected to be Cu-SCR due to its ability to handle the low engine out temperatures. Assuming an ammonia to NO_x ratio of 1, the cumulative NO_x results for engine out, SCR out, and ASC out are shown in Figure 15. The simulation was initialized with zero NH₃ adsorption on the SCR and iterated four times until a pseudo steady state of adsorbed NH₃ is reached. The results shown are from the last, fifth cycle.

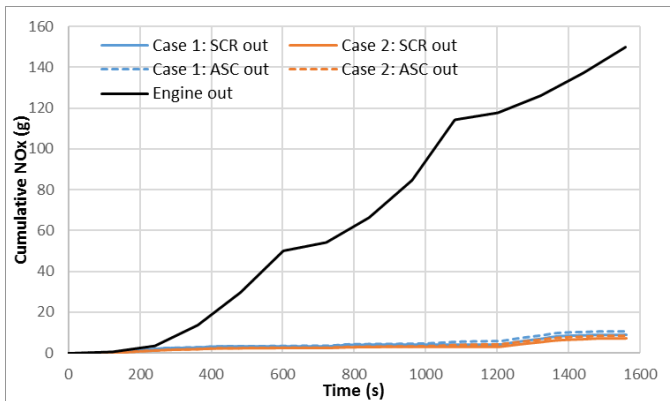


Figure 15: Cumulative NO_x for engine out, SCR out, and ASC out

The results show that more than 96% NO_x conversion can be achieved; however, slight NO_x remake is exhibited in the ASC due to ammonia slip as shown in Figure 16.

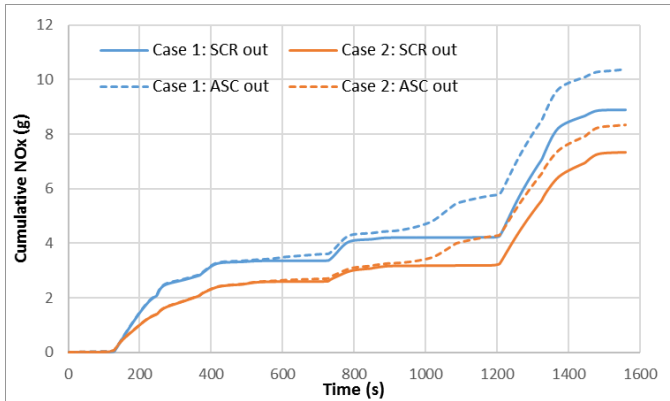


Figure 16: Magnified version of Figure 15 highlighting the NO_x remake from NH₃ slip

Ammonia slip occurs during SCR temperature excursions above 300°C, when ammonia desorbs from the catalyst as shown in Figure 17. Case 1, where there is lower Pt:Pd loading, experiences higher ammonia slip than Case 2 due to a lower NO₂/NO_x ratio, resulting in a slower SCR reaction. The higher NO₂/NO_x ratio of Case 2 utilizes the faster SCR reaction and prevents ammonia slip due to higher consumption rates. However, the higher NO₂/NO_x ratio also leads to increase N₂O production as seen in Figure 18.

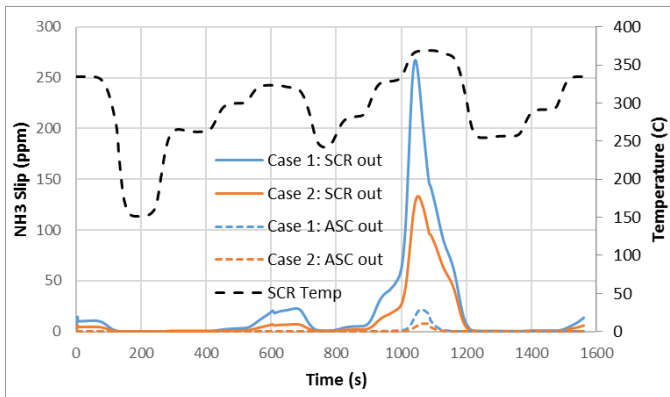


Figure 17: Ammonia slip in SCR and ASC over the 13-mode SET cycle

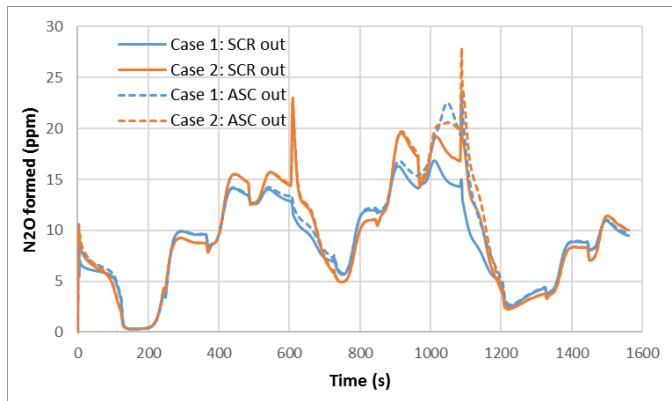


Figure 18: N₂O production over the SET cycle

Table 4: Engine out and tailpipe emissions for 13-mode SET cycle

	Engine out (g/kWh)	Tailpipe (g/kWh)		Standard (g/kWh)
		Case 1	Case 2	
CO	1.264	0	0	-
THC	0.102	0.011	0.008	0.187
NO _x	3.47	0.138	0.120	0.268
N ₂ O	0	0.103	0.112	0.134

The overall emissions from the steady state 13-mode SET cycle are shown in Table 4, which clearly shows that the CO, THC, and NO_x standards can be met with the proposed after-treatment system. However, real world driving requires transient engine operation. The following section describes transient testing performed on the OP Engine over the U.S. heavy-duty Federal Test Procedure (FTP).

Multi-Cylinder Transient Results

The U.S. heavy-duty FTP transient test (Figure 19) was performed on the A48-316, described in [2], and only the hot start results will be presented. The FTP includes a motoring segment requiring the use of a DC or AC dynamometer; however, the dynamometer at Achates Power is an eddy-current unit that is only capable of absorbing power. Therefore, during the motoring section of the cycle, 10% of maximum brake torque relative to the engine speed is commanded resulting in additional fuel consumption and diminished BSFC.

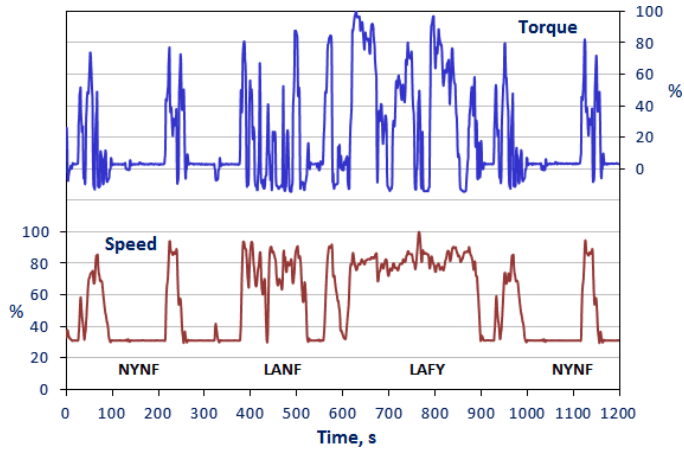


Figure 19: U.S. Heavy-duty FTP transient cycle, reproduced from [19]

The criteria for validating the FTP cycle are shown in Table 5.

Table 5: Statistical requirements for validating FTP cycle

Parameter	Torque	Speed	Power
Slope of regression line, a_1	$0.83 \leq a_1 \leq 1.03$	$0.95 \leq a_1 \leq 1.03$	$0.83 \leq a_1 \leq 1.03$
Absolute value of intercept, $ a_0 $	$\leq 2\%$ of maximum mapped torque	$\leq 10\%$ of warm idle	$\leq 2\%$ of maximum mapped power
Standard Error of Estimate, SEE	$\leq 10\%$ of maximum mapped torque	$\leq 5\%$ of maximum test speed	$\leq 10\%$ of maximum mapped power
Coefficient of Determination, R^2	≥ 0.850	≥ 0.970	≥ 0.910

The minimum engine speed (idle) is 800 RPM and the maximum engine speed is 2200 RPM.

The statistical results from the FTP cycle are shown in Figure 20. The Coefficient of Determination (COD) or R^2 value for brake torque, speed, and power all satisfy the requirements for validating the FTP cycle, confirming the ability of the Achates Power Opposed-Piston Engine to match driver demand.

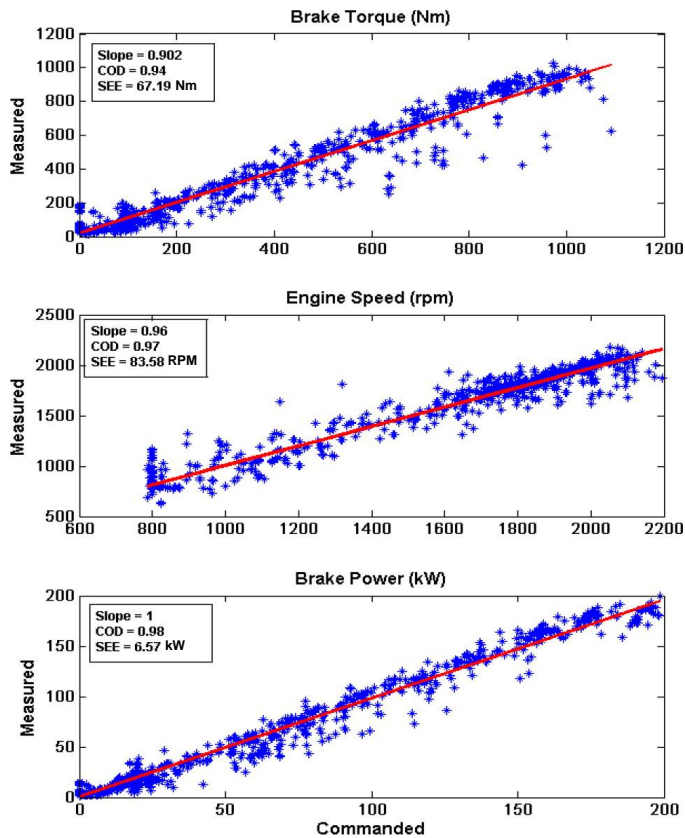


Figure 20: Statistical results for the A48-316 engine on the FTP cycle

The engine-out brake-specific FTP cycle values are shown in Table 6.

Table 6: Hot start FTP cycle average BSFC, engine out BSSoot, engine out BSNO_x

BSFC (g/kWh)	Engine out BSSoot (g/kWh)	Engine out BSNO _x (g/kWh)
217.3	0.056	4.3

FTP measurements were compared to a MY2011 Cummins ISB 6.7L engine highlighted in [20]. Table 7 shows that the Cummins engine performance ratings are similar to the 4.9L Achates Power Opposed-Piston Engine, noting that the Cummins engine was equipped with a DPF and SCR system while the Achates Power OP Engine utilizes a valve to simulate conventional after-treatment back pressures based on supplier input.

Table 7: Comparison of performance specifications between Achates Power Opposed-Piston Engine and MY2011 Cummins 6.7L ISB

	Achates Power OP Engine	MY2011 Cummins MD Engine
Displacement (L)	4.9	6.7
Rated Power (kW)	205	242.5
Rated Speed (RPM)	2200	2400

Peak Torque (Nm) @ Speed	1100 Nm @ 1200 – 1600 RPM	1016 @ 1600 RPM
Compression Ratio	15.4:1	17.3:1
EGR	HP cooled	HP cooled
After-treatment System	Exhaust pressure simulating DPF/DOC/SCR for MD engine	DPF – SCR

Results of the Cummins ISB over the hot start FTP are shown in [20]. A similar amount of work was performed during the cycle, as shown in Table 8, however the total fuel consumed for the Achates Power OP Engine is 20% lower than the Cummins engine with 18% better cycle average BSFC for the Achates Power OP Engine due in part to operation over a much flatter fuel map, as shown in Figure 21.

Table 8: Hot start FTP cycle Achates Power OP Engine compared to MY2011 Cummins 6.7L ISB

	Achates Power OP Engine	MY2011 Cummins MD Engine	Difference
Total energy generated over the cycle (kWh)	14.73	15.30	-0.57
Total fuel consumed (kg)	3.201	4.00	-0.799
BSFC (g/kWh)	217.3	261.4	-44.1

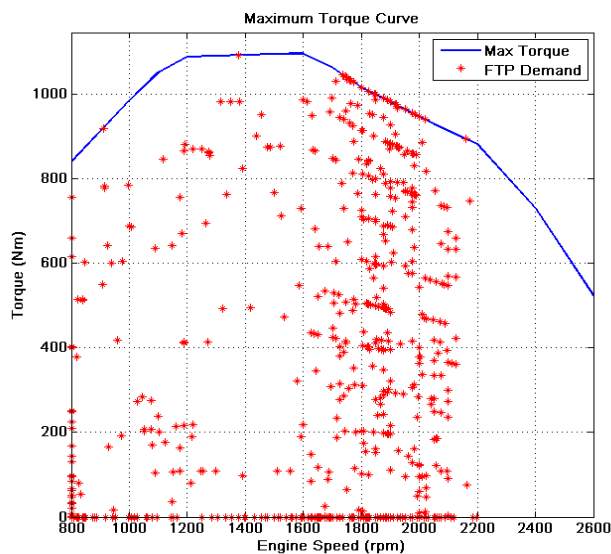


Figure 21: Drive cycle visitation points on OP Engine map

The successful validation of the U.S. heavy-duty FTP transient cycle highlights the excellent drivability of the OP Engine while significantly reducing fuel consumption. To expand the applicability of the OP Engine technology beyond medium and heavy-duty applications, a light-duty study is presented next.

Light-Duty Opposed-Piston Engine

A light-duty version of the OP Engine is described in [3] and is reproduced in Table 9, with a CAD rendering shown in Figure 22.

Table 9: Achates Power Opposed-Piston light-duty truck engine configuration

Cylinder Arrangement/Number	Inline 3
Number of Pistons	6
Number of Injectors	6
Swept Volume/Engine (L)	2.25
Bore (mm)	75.75
Stroke (mm)	166.65
Stroke/Bore Ratio (-)	2.2
Nominal Power ((kW@RPM)	150@3600
Max. Torque (Nm)(Nm@RPM)	500@1600-2100
Emission Standard	Tier 3 LEV III Bin 30



Figure 22: CAD rendering of Achates Power Opposed-Piston light-duty truck engine

GT-Power simulation results for the multi-cylinder light-duty engine were generated using measured single cylinder data (Figure 23), which optimized emissions, combustion noise, temperatures, and efficiency.

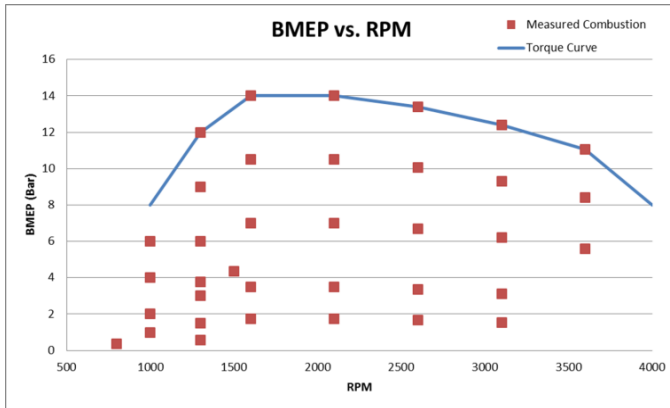


Figure 23: Measured points for input into 1D light-duty engine model

The results for the light-duty engine are shown in Figure 24, Figure 25, and Figure 26. The BSFC (Figure 24) map is extremely flat, generating a best point efficiency greater than 44% from 1600 – 2100 RPM. BSNO_x is maintained close to 1 g/kWh in the FTP cycle operating range with the use of EGR (Figure 25). Using the same after-treatment device as cited in [21], Tier 3 or LEVIII Bin 30 NO_x can be achieved. Likewise, the BSSoot is also extremely low throughout the map and especially in the FTP operating range.

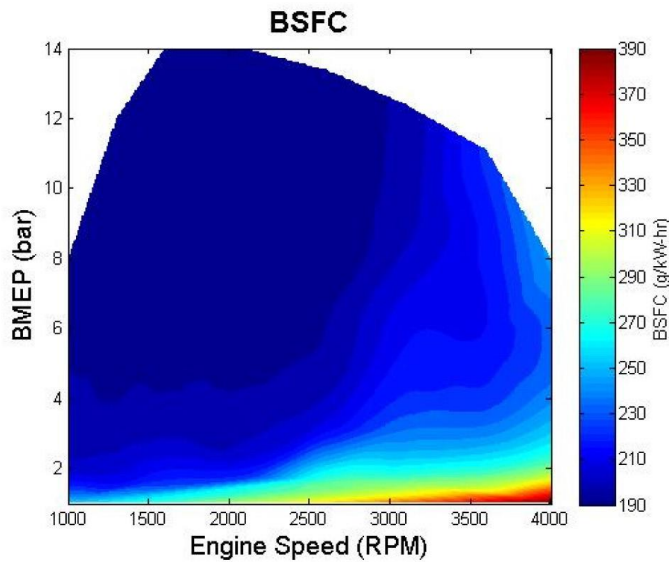


Figure 24: Light-duty BSFC map

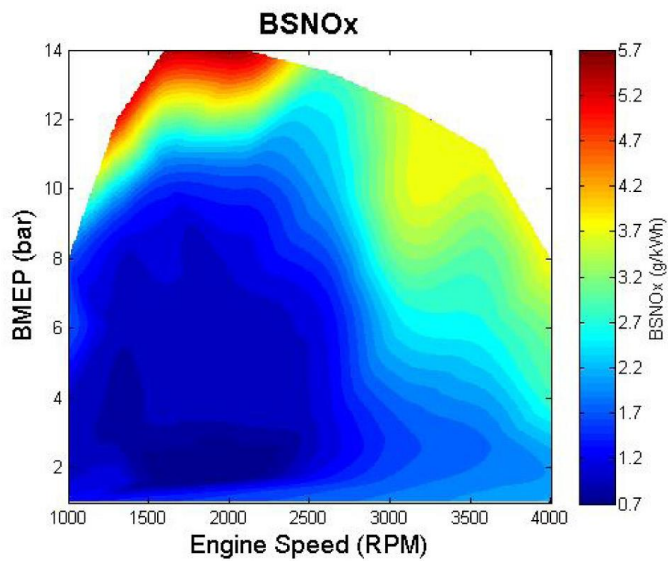


Figure 25: Light-duty BSNOx map

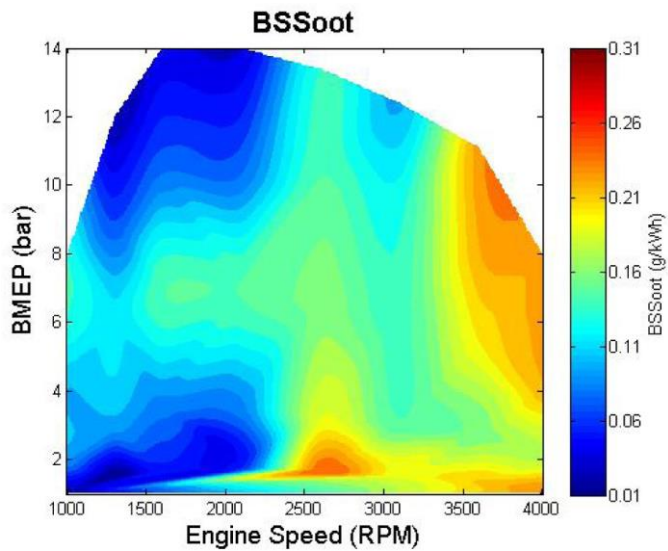


Figure 26: Light-duty BSSoot map

The vehicle cycle fuel economy derived from this exercise was compared to the Cummins ATLAS project results and showed a significant improvement in fuel consumption, NO_x, and PM as can be seen over the LA4 (Table 10) and Highway (Table 11) fuel economy cycles [3, 21].

Table 10: LA4 engine out cycle results *only measured soot with AVL415S not total PM.

Cycle	LA4			
Parameter	Fuel consumption	NOx	PM	HC
Unit	Liter/100 km	g/km	g/km	g/km
Cummins Atlas	8.81	0.51	0.08	-

API OP6	6.89	0.29	0.018	0.075 (THC)
% Improv.	28%	42%	74%	-

Table 11: Highway engine out cycle results *only measured soot with AVL415S not total PM

Cycle	HFET			
	Fuel consumption	NOx	PM	HC
Unit	Liter/100 km	g/km	g/km	g/km
Cummins Atlas	6.83	0.58	0.056	0.062 (NMHC)
API OP6	5.14	0.21	0.025	0.074 (THC)
% Improv.	33%	63%	55%	-16%

The light-duty OP Engine reduced fuel consumption on the order of 30% while drastically reducing NO_x and PM emissions relative to an advanced, state-of-the-art four-stroke diesel research engine. The OP Engine is ideally suited for the light-duty engine sector; the ability of the two-stroke OP Engine to control pumping losses, cylinder scavenging, EGR, internal residuals, and trapped air-fuel ratio results is key for reducing real world fuel consumption. Looking forward, gasoline compression ignition (GCI) has the potential to offer low fuel consumption at low cost.

Opposed-Piston Gasoline Compression Ignition

Achates Power, together with Argonne National Laboratory and Delphi, recently received funding from the U.S. Department of Energy ARPA-E to develop an Opposed-Piston Gasoline Compression Ignition (OPGCI) light-duty engine (DE-AR0000657) [4]. The engine will be a three-cylinder, 2.7L design configured for large passenger vehicles, pickup trucks, SUVs, and vans. The OPGCI engine has the potential to be more than 50% more efficient than a contemporary gasoline engine by combining the benefits of compression ignition with a readily available fuel source – gasoline – in the highly efficient Achates Power OP Engine architecture.

Gasoline is a superior fuel for compression ignition because gasoline is more volatile than diesel and has a longer ignition delay, enabling the completion of injection before combustion starts to avoid soot-forming equivalence ratios. GCI also achieves NO_x emissions through lower peak combustion temperatures resulting from a mostly lean and evenly distributed air/fuel mixture. GCI does emit higher hydrocarbon (HC) and carbon monoxide (CO) emissions. These emissions, however, can be mitigated with relatively inexpensive oxidation catalysts.

GCI also has a cost advantage over diesel technology, both because of much lower cost after-treatment requirements (GCI engines generally do not need a particulate filter and may not need selective catalyst reduction) and because of much lower-cost fuel system.

Delphi and Argonne have demonstrated that gasoline can be combusted without a spark plug under high compression-ratio, lean conditions, and without throttling. The key is to continually produce precisely controlled pressure, temperature, and fuel-dispersion conditions inside the cylinder. Delphi recently published results of experiments that yield 39.3% MPG improvement in combined city and highway drive cycles for a GCI engine compared to a 2.4L four-cylinder port fuel injected (PFI) engine [22].

GCI requires a stratified charge, with locally lean and rich regions. The OP Engine platform is ideally suited for air/fuel mixture preparation with diametrically opposed dual fuel injectors. Each injector can be individually controlled, with flexibility in injection timing, duration, and pressure in order to create ideal mixture distribution and efficient heat release.

The OP Engine platform is also well suited for low load GCI operation. At low loads, the OP Engine can reduce the supercharger work used to boost the intake manifold pressure. This reduces the pressure differential across the engine, reducing the scavenging of the cylinder, and helps retain hot exhaust gases in-cylinder. At low loads, only a little additional oxygen is required for combustion. This has four benefits:

- reduces the amount of work by the supercharger, improving efficiency
- keeps in-cylinder temperatures high for good combustion stability
- provides a natural or internal EGR effect for low NO_x combustion
- provides high exhaust gas temperatures for catalyst light-off and sustained activity

On the other end, GCI requires compromises at high load in conventional four-stroke engines. For conventional engines, a higher compression ratio is required for GCI operation as well as high levels of air and EGR in order to control combustion. These requirements create high cylinder pressures and can limit the peak load of the engine, at which point calibration tradeoffs may be required to maintain mechanical integrity of the engine at the cost of efficiency and performance. The two-stroke operation of the OP Engine reduces the maximum load of the engine while maintaining performance. In addition, the larger cylinder volume enables faster heat release rates, which yield higher efficiency, without increasing combustion noise. These OP Engine characteristics allow for fewer calibration tradeoffs at high loads.

Summary and Conclusions

The Achates Power A48 OP Engine steady state and transient engine results have demonstrated the potential of the opposed-piston architecture to achieve ultra-high efficiency while maintaining low emissions. Despite higher frictional, air handling, and inertial losses, the research grade test engine achieved a SET cycle average 199 g/kWh with a best point of 190 g/kWh, demonstrating the flat nature of the fuel map. An optimized, fresh design of the engine is expected to deliver 180 g/kWh SET cycle average. The A48-316 OP Engine also successfully validated the hot start FTP cycle, demonstrating the engine's ability to follow transient driver demand. Compared to the MY2011 Cummins 6.7L ISB, the OP Engine consumed 20% less fuel during the hot FTP cycle.

Work with Johnson Matthey has shown that the Achates Power OP Engine can satisfy HC, CO, PM, and NO_x EPA10 emissions over the SET cycle. A higher Pt:Pd ratio DOC appears to be beneficial for NO_x and PM reduction compared to a lower Pt:Pd ratio. Ammonia slip is also reduced for the higher Pt:Pd DOC, however higher N₂O emissions are produced. With appropriate urea dosing, NO_x, ammonia, and N₂O EPA10 emissions compliant levels were achieved.

A light-duty configuration of the OP Engine suggests a fuel consumption of about 6 l/100 km, which is a 30% fuel economy improvement over the Cummins ATLAS project. In addition, the OP Engine out emissions show the potential to meet Tier 3 or LEV III Bin 30 standards with appropriate after-treatment. A light-duty gasoline compression ignition variant is estimated to yield 50% fuel economy improvement over conventional gasoline engines while also producing ultra-low emissions. The combination of OP Engine and GCI technology is a promising cost effective solution to meet future greenhouse gas emissions regulations.

Contact Information

Gerhard Regner
Vice President Performance and Emissions
Achates Power, Inc.
4060 Sorrento Valley Boulevard
San Diego, CA 92121
+1 (858) 535-9920
regner@achatespower.com

Acknowledgements

The authors of this paper would like to thank Johnson Matthey for their support and contribution to the after-treatment study presented in this paper.

References

- [1] Nagar, N., Sharma, A., Redon, F., Sukumar, B., and Walker, A. P., "Simulation and Analysis of After-Treatment Systems (ATS) for Opposed-Piston 2 stroke Engine," in *Emissions 2016*, Troy, MI, 2016.
- [2] Sharma, A. and Redon, F., "Multi-Cylinder Opposed-Piston Engine Results on Transient Test Cycle," 2016. 2016-01-1019, 10.4271/2016-01-1019.
- [3] Redon, F., Kalebjian, C., Kessler, J., Rakovec, N., Headley, J., Regner, G., and Koszewnik, J., "Meeting Stringent 2025 Emissions and Fuel Efficiency Regulations with an Opposed-Piston, Light-Duty Diesel Engine," 2014. SAE 2014-01-1187, DOI: 10.4271/2014-01-1187.
- [4] Redon, F., "Exploring the Next Frontier in Efficiency with the Opposed-Piston Engine," in *SIA Powertrain*, Rouen, France, 2016. R-2016-01-29.
- [5] Herold, R. E., Wahl, M. H., Regner, G., Lemke, J. U., and Foster, D. E., "Thermodynamic Benefits of Opposed-Piston Two-Stroke Engines," 2011. SAE 2011-01-2216, DOI: 10.4271/2011-01-2216.
- [6] Fuqua, K., Redon, F., Shen, H., Wahl, M. H., and Lenski, B., "Combustion Chamber Constructions for Opposed-Piston Engines", 2011, US Patent Application US20110271932.
- [7] Venugopal, R., Abani, N., and MacKenzie, R., "Effects of Injection Pattern Design on Piston Thermal Management in an Opposed-Piston Two-Stroke Engine," 2013. SAE 2013-01-2423, DOI: 10.4271/2013-01-2423.
- [8] Regner, G., Johnson, D., Koszewnik, J., Dion, E., Redon, F., and Fromm, L., "Modernizing the Opposed Piston, Two Stroke Engine for Clean, Efficient Transportation," 2013. 2013-26-0114, 10.4271/2013-26-0114.
- [9] Pohorelsky, L., Brynych, P., Macek, J., Vallaude, P.-Y., Ricaud, J.-C., Obernesser, P., and Tribotté, P., "Air System Conception for a Downsized Two-Stroke Diesel Engine," 2012. 2012-01-0831, 10.4271/2012-01-0831.
- [10] Ostrowski, G., Neely, G. D., Chadwell, C. J., Mehta, D., and Wetzel, P., "Downspeeding and Supercharging a Diesel Passenger Car for Increased Fuel Economy," 2012. 2012-01-0704, 10.4271/2012-01-0704.
- [11] Kalebjian, C., Redon, F., and Wahl, M. H., "Low Emissions and Rapid Catalyst Light-Off Capability for Upcoming Emissions Regulations with an Opposed-Piston, Two-Stroke Diesel Engine," in *Emissions 2012 Conference*.
- [12] Teng, H. and Regner, G., "Characteristics of Soot Deposits in EGR Coolers," *SAE Int. J. Fuels Lubr.*, vol. 2, no. 2, pp. 81-90, 2009.
- [13] Scott Sluder, C., Storey, J. M. E., Lewis, S. A., and Lewis, L. A., "Low Temperature Urea Decomposition and SCR Performance," 2005. SAE 2005-01-1858, DOI: 10.4271/2005-01-1858.
- [14] Ahmadinejad, M., Desai, M. R., Watling, T. C., and York, A. P. E., "Simulation of automotive emission control systems," in *Advances in Chemical Engineering*. vol. Volume 33, B. M. Guy, Ed.: Academic Press, 2007, pp. 47-101.
- [15] York, A. P. E., Ahmadinejad, M., Watling, T. C., Walker, A. P., Cox, J. P., Gast, J., Blakeman, P. G., and Allansson, R., "Modeling of the Catalyzed Continuously Regenerating Diesel Particulate Filter (CCR-DPF) System: Model Development and Passive Regeneration Studies," 2007. 2007-01-0043, 10.4271/2007-01-0043.
- [16] Markatou, P., Dai, J., Johansson, A., Klink, W., Castagnola, M., Watling, T. C., and Tutuianu, M., "Fe-Zeolite SCR Model Development, Validation and Application," 2011. 2011-01-1304, 10.4271/2011-01-1304.

- [17] Sukumar, B., Dai, J., Johansson, A., Markatou, P., Ahmadinejad, M., Watling, T., Ranganath, B., Nande, A., and Szailer, T., "Modeling of Dual Layer Ammonia Slip Catalysts (ASC)," 2012. 2012-01-1294, 10.4271/2012-01-1294.
- [18] Ullah, U., Waldram, S. P., Bennett, C. J., and Truex, T., "Monolithic reactors: mass transfer measurements under reacting conditions," *Chemical Engineering Science*, vol. 47, no. 9, pp. 2413-2418, 1992.
- [19] https://www.dieselnet.com/standards/cycles/ftp_trans.php. Accessed October 4, 2016.
- [20] Thiruvengadam, A., Pradhan, S., Thiruvengadam, P., Besch, M., Carder, D., and Delgado, O., "Heavy-Duty Vehicle Diesel Engine Efficiency Evaluation and Energy Audit," The International Council on Clean Transportation October 2014.
- [21] Suresh, A., Langenderfer, D., Arnett, C., and Ruth, M., "Thermodynamic Systems for Tier 2 Bin 2 Diesel Engines," *SAE Int. J. Engines*, vol. 6, no. 1, pp. 167-183, 2013.
- [22] Sellnau, M., Sinnamon, J., Hoyer, K., and Husted, H., "Gasoline Direct Injection Compression Ignition (GDCI) - Diesel-like Efficiency with Low CO₂ Emissions," *SAE Int. J. Engines*, vol. 4, no. 1, pp. 2010-2022, 2011.